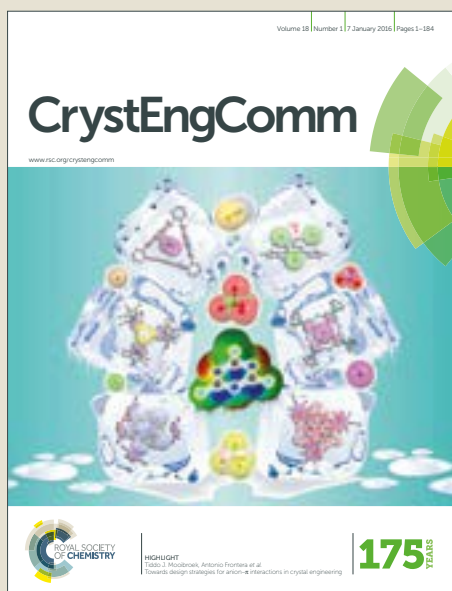


CrystEngComm

Accepted Manuscript



This article can be cited before page numbers have been issued, to do this please use: Z. Bai, Y. Zheng, W. Han, Y. Ji, T. Yan, Y. Tang, G. Chen and Z. Zhang, *CrystEngComm*, 2018, DOI: 10.1039/C8CE00808F.



This is an Accepted Manuscript, which has been through the Royal Society of Chemistry peer review process and has been accepted for publication.

Accepted Manuscripts are published online shortly after acceptance, before technical editing, formatting and proof reading. Using this free service, authors can make their results available to the community, in citable form, before we publish the edited article. We will replace this Accepted Manuscript with the edited and formatted Advance Article as soon as it is available.

You can find more information about Accepted Manuscripts in the [author guidelines](#).

Please note that technical editing may introduce minor changes to the text and/or graphics, which may alter content. The journal's standard [Terms & Conditions](#) and the ethical guidelines, outlined in our [author and reviewer resource centre](#), still apply. In no event shall the Royal Society of Chemistry be held responsible for any errors or omissions in this Accepted Manuscript or any consequences arising from the use of any information it contains.

Cite this: DOI: 10.1039/c0xx00000x

www.rsc.org/xxxxxx

ARTICLE TYPE

Development of Trapezoidal MgO Catalyst for High-Efficient Transesterification of Glycerol and Dimethyl Carbonate†

Zongquan Bai, Yajun Zheng, Weiwei Han, Yue Ji, Tianlan Yan, Ying Tang*, Gang Chen, and Zhiping Zhang*

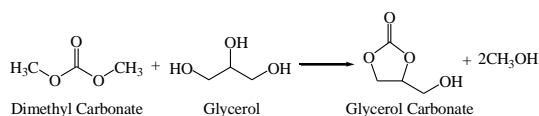
Received (in XXX, XXX) Xth XXXXXXXXX 20XX, Accepted Xth XXXXXXXXX 20XX

DOI: 10.1039/b000000x

A series of micro-sized MgO with various morphologies have been prepared by varying the reaction temperature and stirring time during precipitation, and were investigated for the production of glycerol carbonate from the transesterification of glycerol with dimethyl carbonate. In contrast to other morphologies of MgO (e.g., rod-like, spherical, flower-like and nest-like), trapezoidal MgO demonstrated a superior performance with a yield of glycerol carbonate more than 99%. Various techniques including N₂ physical adsorption, XRD, CO₂ chemical adsorption and EDS revealed that the unique catalytic activity of trapezoidal MgO was related to its lower specific surface area, bigger crystallite size, weaker surface basicity and less Mg atom vacancies compared to other morphologies of MgO. The experimental conditions (e.g., catalyst amount, solvent, reaction temperature and the molar ratio between glycerol and dimethyl carbonate) were also found playing crucial roles in determining the yield of glycerol carbonate. Furthermore, CO₂-TPD profile and FT-IR spectra indicated that the weak surface basic sites occurred at 150 °C and the CO₃²⁻ stretching vibration around 1448 cm⁻¹ were responsible for the catalytic activity of developed trapezoidal MgO in regeneration.

1. Introduction

As a high value-added glycerol derivative, glycerol carbonate has been applied as solvent, electrolytes liquid carrier, cement and concrete, liquid membrane, chemical intermediate and so on because of its special properties such as high boiling point, low melting point, dielectric constants close to the one of water and low toxicities¹⁻⁴. However, its market price is greater than 8,141 dollar/ton⁴, which greatly limits its usage in various fields (only a few kilotons per year)². To address this issue, different synthetic routes²⁻⁷ have been developed to prepare glycerol carbonate. The most used route is through the transesterification of dimethyl carbonate and glycerol (**Scheme 1**) in terms of its mild reaction conditions, high glycerol carbonate reaction yield and environmentally benign^{8, 9}. In the synthesis, catalyst plays a significant role in determining the reaction efficiency. Taking into account the high boiling temperature of both glycerol and glycerol carbonate, a heterogeneous catalyst is preferred for the production of glycerol carbonate. Up to now, various heterogeneous base catalysts, including CaO^{6, 10}, MgO^{8, 11}, Mg/La mixed oxide¹², Mg/Al hydrotalcite⁹, Mg_{1.2}Ca_{0.8}O₂ mixed oxide¹³, Mg/Zr/Sr mixed oxide¹⁴ and Mg/Al/Zr mixed oxide¹⁵, have been receiving more considerable attention than acidic ones because the latter gives poor reaction performance resulting from the limitation of mass transport⁴. Among the heterogeneous base catalysts, MgO demonstrated a low catalytic activity with only around 10% glycerol carbonate yield^{9, 15, 16} attributable to its weakest basic strength among group II oxides¹⁷⁻¹⁹.



Scheme 1. Synthesis of glycerol carbonate from dimethyl carbonate and glycerol.

As reported in numerous studies²⁰⁻²⁶, the catalytic performance of MgO was heavily dependent on its morphology. For example, Zhang et al.²⁵ reported that parallelogram-like mesocrystal MgO had superior catalytic performance to trapezoidal MgO in the Meerwein–Ponndorf–Verley catalytic reaction between benzaldehyde and ethanol. Sutradhar et al.²¹ observed that the MgO with shapes of flower and house-of-cards demonstrated highly catalytic activity in the condensation reaction between benzaldehyde and acetophenone due to the large amounts of step edges and corners, low coordinated sites and lattice defects in their structures, and the high reactivity of nanoflake MgO was attributable to their high surface area. Li and Shen²⁶ comprehensively reviewed the important progress on the morphology-dependent phenomenon of rod-shaped metal oxides with characteristic redox and acid-base features. To improve the catalytic activity of MgO in the transesterification of glycerol and dimethyl carbonate, Simanjuntak et al.⁸ compared three morphologies of MgO (e.g., flake-like, irregular and spherical-like), and found that spherical-like MgO synthesized using a Pluronic P127 surfactant exhibited the highest activity. A glycerol carbonate yield as high as 75.4% was obtained owing to its higher basic site concentration on the surface.

Inspired by those reports, herein we prepared a series of micro-sized MgO with trapezoidal, rod-like, spherical, flower-like and nest-like structures in the temperature range of 30 - 80 °C via precipitation approach employing Mg(NO₃)₂, Na₂CO₃ and Na₂C₂O₄ as raw materials^{25, 27-30}. Their catalytic activities for the transesterification between glycerol and dimethyl carbonate were compared. To elucidate the high catalytic activity of trapezoidal MgO (more than 99% of yield), various techniques, including X-ray diffraction, N₂ physical adsorption and CO₂ chemical adsorption, were employed to characterize the MgO with different morphologies. In addition, the influences of experimental parameters (e.g., catalyst amount, solvent, reaction temperature,

the molar ratio between glycerol and dimethyl carbonate, reaction time and reusability) on the yield of glycerol carbonate were studied in detail.

Table 1. Experimental parameters for preparation of the MgO with different morphologies

Morphology	Magnesium Salt	Precipitant	Reaction Temperature (°C)	Stirring Time (min)
trapezoidal	Mg(NO ₃) ₂ ·6H ₂ O	Na ₂ C ₂ O ₄	30	1.5
rod-like	Mg(NO ₃) ₂ ·6H ₂ O	Na ₂ CO ₃	50	1.5
spherical	Mg(NO ₃) ₂ ·6H ₂ O	Na ₂ CO ₃	70	1.5
flower-like	Mg(NO ₃) ₂ ·6H ₂ O	Na ₂ CO ₃	70	3.0
nest-like	Mg(NO ₃) ₂ ·6H ₂ O	Na ₂ CO ₃	80	1.5

2. Experimental

2.1 Catalyst preparation

All reagents including magnesium nitrate [Mg(NO₃)₂·6H₂O], sodium carbonate [Na₂CO₃], and sodium oxalate [Na₂C₂O₄] were of analytical grade or better and used without further purification. In the present study, five morphologies of micro-sized MgO particles were prepared, and **Table 1** lists their experimental parameters. It was interesting to find that as Na₂CO₃ was employed as a precipitant, the experimental parameters such as reaction temperature and stirring time had pronounced effects on the morphology of resulting product. However, little effect was observed when Na₂C₂O₄ was used, and only trapezoidal particles could be obtained.

In a typical synthesis, 10.26 g of Mg(NO₃)₂·6H₂O was dissolved into 50 mL of double-deionized water, which was then transferred into a 250 mL three-necked flask and heated to 30 °C. Afterwards, 100 mL of 0.4 M Na₂C₂O₄ solution was also heated to 30 °C. Under vigorous stirring (*ca.* 800 rpm), the prepared Na₂C₂O₄ solution was poured into the Mg(NO₃)₂ solution in 10 s followed by stirring for 1.5 min. Subsequently, the mixture was maintained at 30 °C for 1 h without stirring, and then the generated product was collected, filtered and washed with double-deionized water and absolute ethanol several times. The MgO sample was fabricated by calcination of the obtained product in air from room temperature to 550 °C in a muffle furnace, and then maintained at that temperature for 3 h.

2.2 Catalyst characterization

The morphology and size of the obtained particles were examined by a JEOL JSM-6390A scanning electron microscope (SEM), and the energy dispersive spectroscopy (EDS) analysis was performed on a Carl Zeiss SIGMA scanning electron microscope. The crystal structures of the as-synthesized products were

characterized by X-ray diffraction (XRD) on a XRD-6000 diffractometer using Cu K_α radiation. The operation voltage was 40 kV, and the current was 30 mA. Nitrogen adsorption–desorption isotherms were obtained using a Micrometrics ASAP 2020HD88 instrument at 77 K. for which the samples were degassed at 200 °C for 12 h before the measurement. The surface area was calculated by the Brunauer-Emmett-Teller (BET) method. Temperature-programmed desorption of CO₂ (CO₂-TPD) was carried out to determine the basicity of the MgO particles using a Micromeritics ChemiSorb 2750 reactor. The IR spectra of the obtained samples were recorded with a Bruker vertex 70 series FT-IR spectrometer in transmission mode in the range of 4000–400 cm⁻¹. The resolution was 4 cm⁻¹ and eight scans were signal-averaged in each interferogram.

2.3 Catalyst evaluation

The catalysts were evaluated by the transesterification reaction between glycerol and dimethyl carbonate. Specifically, glycerol, dimethyl carbonate and absolute ethanol with a molar ratio of 1:3:3 (the weight of glycerol was 10.0 ± 0.5 g) were added into a 100 mL round-bottomed flask having reflux condenser. After a stirring time of 5.0 min for thorough mixture, MgO catalyst with a weight of 3% glycerol was added into the reaction solution. The mixture was heated with stirring at a desired temperature using bath oil. After the reaction, the catalyst was separated from the reaction mixture using centrifugation separation. The collected products were analyzed with an GC-2000 gas chromatograph (Focused Photonics Inc., Hangzhou, China) equipped with a DB-Wax capillary column (30 m × 0.32 mm I.D., 0.25 μm film thickness) and a FID detector. The carrier gas was nitrogen with a flow rate of 20 mL min⁻¹. The yield of glycerol carbonate in reaction production was calculated using internal standard method, in which butanol was as the internal standard.

3. Results and Discussion

3.1 Preparation and catalytic characterization of MgO particles with various morphologies. According to our previous reports^{25, 27–30}, five types of MgO particles with trapezoidal, rod-like, spherical, flower-like and nest-like structures were prepared via the reaction between Mg(NO₃)₂ and Na₂C₂O₄ or Na₂CO₃ by varying the experimental parameters such as reaction temperature and stirring time as listed in **Table 1**. **Figure 1** shows the typical SEM images of obtained MgO particles by calcining their precursors at 550 °C for 3 h. As Mg(NO₃)₂ and Na₂C₂O₄ were used as the raw materials at the reaction temperature of 30 °C, trapezoidal MgO with a topline width of *ca.* 3.4 μm, baseline width of *ca.* 8.6 μm

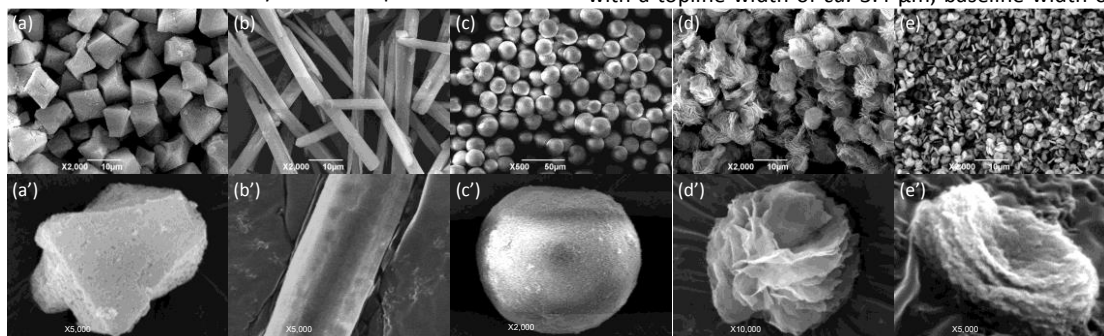


Figure 1. SEM images of different morphologies of MgO particles: (a) and (a') trapezoidal MgO, (b) and (b') rod-like MgO, (c) and (c') spherical MgO, (d) and (d') flower-like MgO, and (e) and (e') nest-like MgO, in which (a), (b), (c), (d) and (e) are the panoramic morphology, and (a'), (b'), (c'), (d') and (e') are the individual particle.

and height of *ca.* 8.6 μm were obtained (**Figure 1a** and **a'**), in agreement with the previous report²⁵. When $\text{Mg}(\text{NO}_3)_2$ and Na_2CO_3 were employed for reaction at a temperature of 50 $^\circ\text{C}$, rod-like MgO particles with an average diameter of 4.1 μm were achieved, and their length was in the range of 41.2 - 63.8 μm (**Figure 1b** and **b'**). With increase in the reaction temperature from 50 to 70 $^\circ\text{C}$, spherical MgO with an average diameter of 22.8 μm could be obtained (**Figure 1c** and **c'**). Under the same reaction temperature as the spherical MgO precursor but different stirring time (3.0 min), flower-like MgO with a diameter of around 6.5 μm could be achieved (**Figure 1d**). The particles were composed of layer-like structures, and the thickness of each layer was around 50 nm (**Figure 1d'**). This fact might result from the prolonged vigorous stirring, which disturbed the self-assembly orientation of MgO precursor. Thus different morphologies of products were generated with variation in stirring time. As the reaction temperature increased up to 80 $^\circ\text{C}$, nest-like MgO particles were obtained, and their average length, width and height were 3.17, 2.26 and 0.83 μm , respectively (**Figure 1e**). Careful observation could be found that the particle was composed of layer-like structure, and the thickness of each layer was about 120 nm (**Figure 1e'**). From the above discussion, it is obvious that the experimental parameters have a great effect on the shape of resulting MgO. As reported in the literature²⁰⁻²⁶, the catalytic performance of MgO was closely related to its morphology. To evaluate the catalytic activity of the obtained MgO with various morphologies, dimethyl carbonate and glycerol were used as reactants, ethanol was employed as solvent. **Figure 2** shows the yield of glycerol carbonate after a reaction period of 1 h at 70 $^\circ\text{C}$. Apparently, as trapezoidal MgO particles were used as catalyst, the yield of glycerol carbonate was as high as 93.0%. However, the catalytic performances were comparable for other morphologies of MgO (e.g., rod-like, spherical, flower-like and nest-like structures), and the yields were all below than 6.5%. These results illustrate the catalytic activity of MgO is highly dependent on its shape, in consistent with the previous reports²⁰⁻²⁶.

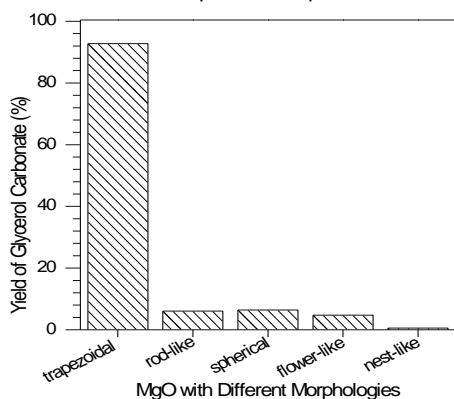


Figure 2. Comparison of the catalytic activities of MgO with various morphologies in the transesterification of dimethyl carbonate and glycerol into glycerol carbonate (Note: reaction temperature, 70 $^\circ\text{C}$; reaction time, 1 h).

3.2 Correlation between the catalytic activity of MgO and their physicochemical properties. To get an insight into the catalytic activities of the MgO with different morphologies and their physicochemical properties, various techniques were employed to characterize the surface properties of obtained MgO particles.

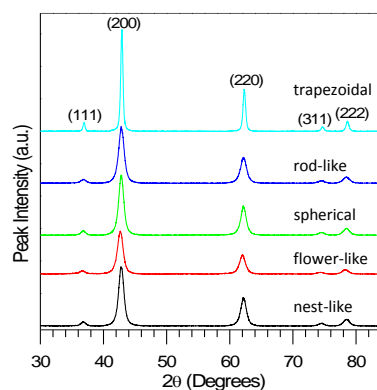


Figure 3. XRD patterns of the generated MgO with various morphologies as indicated.

Their porosities were obtained from the N_2 adsorption isotherms. As listed in **Table 2**, the specific surface areas of obtained MgO changed significantly with variation in their morphologies. For the trapezoidal MgO, its specific surface area was as low as 31.8 $\text{m}^2 \text{g}^{-1}$, whereas the values were in the range of 116.2 – 160.1 $\text{m}^2 \text{g}^{-1}$ for the MgO with rod-like, spherical, flower-like and nest-like structures. After comparing with their catalytic performances (**Figure 2**), no direct correlation was found between the specific surface area and the catalytic capacity. In addition, the average pore diameter and pore volume were not directly related to the catalytic performance of generated MgO. Careful observation could be found that the specific surface area and pore volume of the trapezoidal MgO are much lower than those of others, whereas it demonstrates the highest catalytic capacity. As reported in many studies³¹⁻³⁵, a higher specific surface area and pore architecture would lead to a more favorable catalytic performance. The opposite case in the current study suggests that those parameters are not the dominant factors in determining the catalytic performance of generated MgO with different morphologies.

Figure 3 shows the XRD patterns of the generated MgO with different morphologies. Obvious diffraction peaks of cubic phase of MgO with a lattice constant of $a = 4.21$ can be seen in all samples, in good agreement with the reported value in the literature (JCPDS no. 45-0946). In addition, it could be seen that with variation in the morphology of generated MgO, the intensity of diffraction peaks has some differences. For the trapezoidal MgO, it illustrates the most intensive and the sharpest diffraction peaks in contrast to the MgO with rod-like, flower-like, spherical and nest-like structures. For the latter, their diffraction peaks are comparable, which suggests that they should have similar crystallite sizes. After calculation using Debye-Scherrer formula based on the full width

Table 2. Texture properties of as-synthesized MgO particles

Morphology	Specific surface area ($\text{m}^2 \text{g}^{-1}$) ^[a]	Average pore diameter [nm] ^[b]	Pore volume [$\text{cm}^3 \text{g}^{-1}$]	Crystallite size (nm) ^[c]
trapezoidal	31.8	19.5	0.13	23.1
rod-like	160.1	5.7	0.34	9.0
spherical	136.1	12.3	0.58	8.2
flower-like	116.2	11.4	0.38	8.8
nest-like	141.8	11.3	0.49	8.1

Note: ^[a] Using the standard Brunauer-Emmett-Teller (BET) method; ^[b] Using the Barret-Joyner-Halenda (BJH) method; ^[c] Using Debye-Scherrer formula based on the full width at half-maximum (fwhm) of (200) plane.

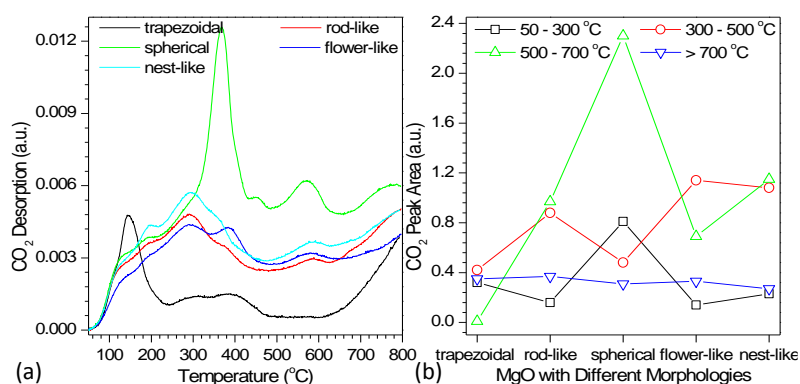


Figure 4. (a) CO₂-TPD profile of the generated MgO with various morphologies as indicated and (b) the variation in the peak areas in different temperature regions with their morphologies.

at half-maximum (fwhm) of (200) plane, the crystallite size for the trapezoidal MgO is as high as 23.1 nm, whereas the values are in the range of 8.1 – 9.0 nm for other MgO particles as listed in **Table 2**. According to those results, it is interesting to conclude that for the studied MgO, the bigger the crystallite size of generated MgO, the more the catalytic activity (**Figure 2**).

As reported in the previous studies^{9, 15, 16}, MgO demonstrated a low catalytic activity attributable to its weakest basic strength among group II oxides¹⁷⁻¹⁹. To get an insight into the correlation between the catalytic performance of generated MgO and their basic properties, the surface basicity of collected MgO particles was examined by the temperature-programmed desorption (TPD) of CO₂. As shown in **Figure 4a**, the surface basic properties of obtained MgO varied significantly with variation in their morphologies. Among the studied products, the trapezoidal MgO illustrated the weakest basicity, and there was a sharp CO₂ desorption peak centered around 155 °C. For the MgO with rod-like, flower-like and nest-like structures, they showed a stronger surface basicity than that of trapezoidal MgO, whereas the abundance of CO₂ desorption peaks were comparable, suggesting that they had a similar surface basic property. For spherical MgO, it illustrated the strongest basicity, and there was an intensive CO₂ desorption peak around 370 °C. According to those results, it was obvious that the catalytic activity of generated MgO had little correlation with their surface basicity, not in agreement with the previous reports^{9, 15, 16}.

Careful observation could also be found that with variation in the morphology of the MgO, these desorption peaks could be divided into four groups exhibiting weak (CO₂ desorption in the range of 50 - 300 °C), medium (CO₂ desorption in the range of 300 - 500 °C), strong (CO₂ desorption in the range of 500 - 700 °C) and super basicity (CO₂ desorption above 700 °C), which was similar to our recent report³⁶ but different from the previous reports^{30, 37, 38} with only three types of basic sites in an order of low coordination oxygen anions > oxygen in Mg²⁺ and O²⁻ pairs > hydroxyl groups at the surface of MgO. According to the results, we quantitatively described the correlation between the areas of CO₂ desorption peaks at different temperature ranges and the MgO morphology as

shown in **Figure 4b**. It was clear that in the temperature range of 50 – 300 °C, the CO₂ desorption peak of spherical MgO demonstrated the highest value, which was 2.5 – 5.8-fold higher than those of other MgO. In the range of 300 – 500 °C, both trapezoidal and spherical MgO illustrated comparable values, which were 2.1 – 2.7-fold lower than rod-like, flower-like and nest-like MgO. As the temperature was increased to 500 – 700 °C, trapezoidal MgO exhibited the lowest value followed by rod-like, flower-like and nest-like MgO, whereas spherical MgO showed the highest value, which was 230-fold higher than that of trapezoidal MgO. However, comparable values were obtained for all of the studied MgO as the temperature was increased above 700 °C. Despite this, no direct relationship was observed between the surface basicity of obtained MgO and their catalytic performances.

According to many experimental evidence and model calculations³⁹⁻⁴³, there were different oxygen vacancies at the surface or sub-surface region of MgO. It is different from other covalent oxides, and the removal of oxygen atoms in the structures of MgO will not lead to the formation of new bonds but rather cavities, which might be responsible to the different catalytic performances of the MgO with various morphologies in the current study. To confirm this assumption, the contents of O atom and Mg atom in the structures of obtained MgO with different morphologies were analyzed using EDS measurement. As shown in **Figure 5a**, with variation in the morphologies of obtained MgO, the percentages of Mg and O atoms in their structures changed significantly. But different from the above assumption, the content of O atom (ranging from 50.4 - 55.5%) in the structure of MgO was much higher than that of Mg atom (changing from 44.5% to 49.6%). This fact reveals that there are a certain amount of Mg atom vacancies in the generated MgO with different morphologies. Careful examination could be found that among them, trapezoidal MgO had an equivalent ratio between O and Mg (namely 1.02), whereas for other morphologies of MgO, the ratio changed from 1.11 to 1.25. According to the report by Simanjuntak *et al.*¹⁰, in the transesterification reaction between glycerol and dimethyl

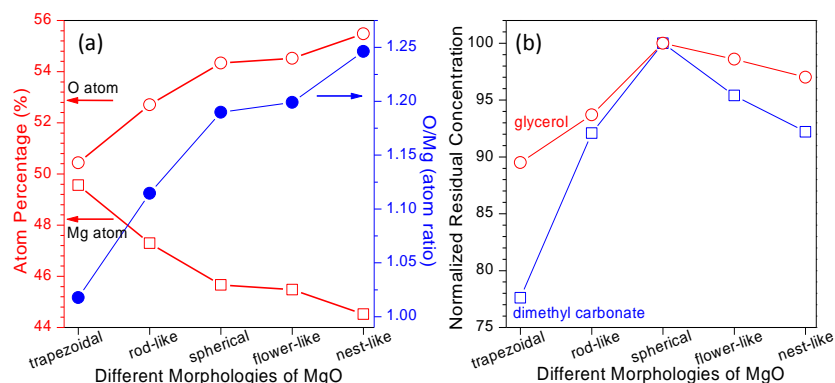


Figure 5. (a) Variation in the percentages of O atom and Mg atom and the ratios between them (O/Mg) in the structures of different morphologies of MgO using EDS analysis ($n = 6$) and (b) the variation in the residual concentrations of glycerol and dimethyl carbonate in centrifuged ethanol solution after mixing 0.1 g different morphologies of MgO and 3.5 g glycerol and 10.37 g dimethyl carbonate in 6.58 mL ethanol at 70 °C for 1 h, respectively.

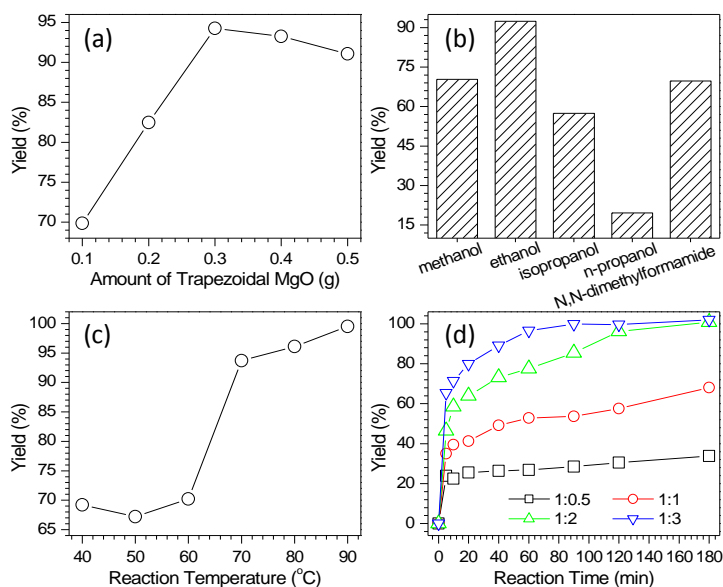


Figure 6. Influences of experimental parameters on the yield of glycerol carbonate over trapezoidal MgO: (a) effect of the added amount of trapezoidal MgO catalyst relative to the content of glycerol, (b) effect of solvent including methanol, ethanol, isopropanol, n-propanol and N,N-dimethylformamide, (c) effect of reaction temperature ranging from 40 to 90 °C, and (d) effect of reaction time and the ratio between glycerol and dimethyl carbonate.

carbonate, the used catalyst CaO would first attack the hydroxyl groups in glycerol followed by the carboxyl groups in dimethyl carbonate, and then the resulting intermediate further reacted with glycerol by production of glycerol carbonate. For the reaction using MgO as catalyst, glycerol and dimethyl carbonate might experience a similar mechanism as that on CaO (Figure S1 and the related discussion). In this process, it could be concluded that the interaction between a solid base catalyst (e.g., CaO and MgO) and glycerol or dimethyl carbonate was crucial in determining the reaction efficiency. If there were more O atoms in a catalyst such as the studied MgO, it would become hard to attack the hydroxyl groups in glycerol followed by the carboxyl groups in dimethyl carbonate owing to a stronger electron repulsion force between MgO and reactants, thus leading to a lower reaction efficiency. On the contrary, a high-efficient transesterification between glycerol and dimethyl carbonate would occur. To get a direct evidence on this, the interaction between the MgO with different morphologies and glycerol and/or dimethyl carbonate was investigated. Figure 5b illustrates the residual content of glycerol and dimethyl carbonate in ethanol after mixing them with various MgO for 1 h at 70 °C. It is apparent that in contrast to other morphologies of MgO, trapezoidal MgO with a lower O:Mg ratio exhibits more favorable interactions with glycerol and dimethyl carbonate, respectively, which results in a lower concentration in the solution. This fact to a certain degree explains why trapezoidal MgO was prone to give a higher reaction efficiency relative to other morphologies of MgO (Figure 2).

3.3 Experimental parameters in determining the catalytic activity of trapezoidal MgO. As reported in the previous study⁴, the yield of glycerol carbonate in transesterification reaction are significantly affected by the reaction parameters. In the present work, we systematically investigated the influences of the amount of trapezoidal MgO catalyst, solvent type, reaction temperature,

reaction time and the molar ratio between glycerol and dimethyl carbonate on the yield of glycerol carbonate. Figure 6a shows the effect of trapezoidal MgO catalyst on the yield of glycerol carbonate. It is apparent that by fixing other parameters, the yield demonstrated a gradually increasing trend followed by keeping almost constant with increase in the added amount of MgO catalyst. As the added amount of trapezoidal MgO was 0.3 g, namely 3% relative to the amount of glycerol, the yield of glycerol carbonate reached the maximum value (around 94.3%), in good agreement with the previous report⁴⁴. Further increasing the catalyst amount led to a slight decrease in the yield probably attributable to the involved side reaction⁴⁵. In the synthesis of glycerol carbonate, addition of solvent is essential to increase the miscibility of glycerol with dimethyl carbonate. Figure 6b shows the effect of various solvents, including methanol, ethanol, isopropanol, n-propanol and N,N-dimethylformamide, on the yield of glycerol carbonate. It is obvious that when n-propanol was used as a solvent, a yield as low as 19.6% was achieved. For methanol, isopropanol and N,N-dimethylformamide, comparable conversion efficiency in the range of 57 – 70% was obtained. As ethanol was used as solvent, the yield reached the maximum value of 92.4%. In the current study, we also found that reaction temperature was a crucial factor in determining the yield of glycerol carbonate. Figure 6c illustrates the variation in the yield with increase of the reaction temperature ranging from 40 to 90 °C. For this figure, it can be seen that when the reaction temperature was in the range of 40 - 60 °C, the reaction yield maintained constant with a value of around 70%. However, as the reaction temperature was increased up to 70 °C, a reaction yield as high as 93.7% was obtained, and further increasing the temperature (80 – 90 °C) led to a slight increase in the reaction yield, in consistent with the previous reports⁴⁵⁻⁴⁸. This phenomenon could be in part due to the fact that a higher reaction temperature would result in an increase in the collision between reactants and thus leading to a higher reaction yield⁴. In the transesterification of glycerol with glycerol carbonate, the product yield is also greatly affected by the molar ratio of reactants. As shown in Figure 6d, as the molar ratio between glycerol and glycerol carbonate was 1:0.5, the yield was only 33.8% even after a reaction time of 180 min. As the ratio became 1:1, the value was improved to 68.1%. Further enhancing the ratio to 1:2, a yield of 96.2% could be achieved after a reaction time of 120 min. When the ratio was 1:3, the reaction efficiency was significantly increased. It is obvious that after a reaction time of 60 min, the yield could be as high as 96.6%, and increasing the reaction period could lead to a reaction efficiency above than 99%. Owing to the high yield, no more ratio was conducted. From the above discussion, it can be seen that the reaction parameters such as the catalyst amount, solvent, reaction temperature and the ratio between reactants are crucial in controlling the final yield of glycerol carbonate over the developed trapezoidal MgO catalyst.

3.4 Reusability of trapezoidal MgO. Reusability is another important consideration in developing a catalyst. In the current study, we found that the yield of glycerol carbonate was pretty low by using the following ways to handle the developed MgO catalyst for recycle: (a) after the reaction between glycerol and dimethyl carbonate, the catalyst was centrifuged, washed with ethanol for

three times, dried at 80 °C and reused for the next reaction, the reaction yield was low as 5.3%; (b) after centrifugation and washing with ethanol for three times, the obtained catalyst was calcined at 300 - 900 °C for 3 h and reused, and the yields were all below 10%; (c) according to on the report by Simanjuntak et al.⁸, after centrifugation, the collected catalyst was first heated to 400 °C and maintained for 3 h in a nitrogen atmosphere followed by calcination at 550 °C for 3 h in air, the yield was as high as 97.4%. As shown in **Figure 7a**, the activity of collected catalyst was maintained at this level after three cycles. To figure out the variation in the surface properties of trapezoidal MgO by calcination in air and in both N₂ and air, we compared the collected catalysts from different conditions. **Figure 7b** illustrates the CO₂-TPD profiles of the generated MgO prior to catalysis, after catalysis and calcination at 550 °C for 3 h in air and after catalysis and calcination at 400 °C for 3 h in a N₂ atmosphere followed by calcination at 550 °C for 3 h in air. From this figure, it is obvious that for the catalyst prior to catalysis, there is a sharp CO₂ desorption peak around 150 °C attributable to the weak basic sites on the MgO surface. However, after one cycle and calcination at 550 °C for 3 h in air, this peak hardly observed although others kept almost constant. However, after one cycle and calcination at 400 °C for 3 h in a N₂ atmosphere followed by calcination at 550 °C for 3 h in air, the peak reoccurred at 150 °C. Meanwhile, as the above discussion, the catalytic activity of collected MgO maintained after treatment with this way. This fact suggests that the basic site may be responsible for the high catalytic performance of trapezoidal MgO. We also used FT-IR spectra to probe the surface variation with experimental conditions. As shown in **Figure 7c**, with change in the treatment conditions, only two bands occurred at 3454 cm⁻¹ (O-H stretching vibration in H₂O) and around 1448 cm⁻¹ (absorbed CO₃²⁻ stretching vibration) took place a great change. It is interesting to observe that for the MgO catalyst after one cycle and calcination at 400 °C for 3 h in a N₂ atmosphere followed by calcination at 550 °C for 3 h in air, the band around 1448 cm⁻¹ maintained almost same as that without use for catalysis, whereas it became much weaker as it was directly calcined at 550 °C for 3 h in air. This case illustrated that the intensity of the band occurred at 1448 cm⁻¹ was probably another indication of the catalytic activity of developed trapezoidal MgO. Despite this, it should be mentioned here that for the products after calcination at 400 °C for 3 h in a N₂ atmosphere and in air, it was favorable to see their appearance difference, but it was hard to distinguish their exact compositions using our available techniques such as FT-IR or XRD techniques (**Figure S2**). Further investigation is still under the way.

4. Conclusions

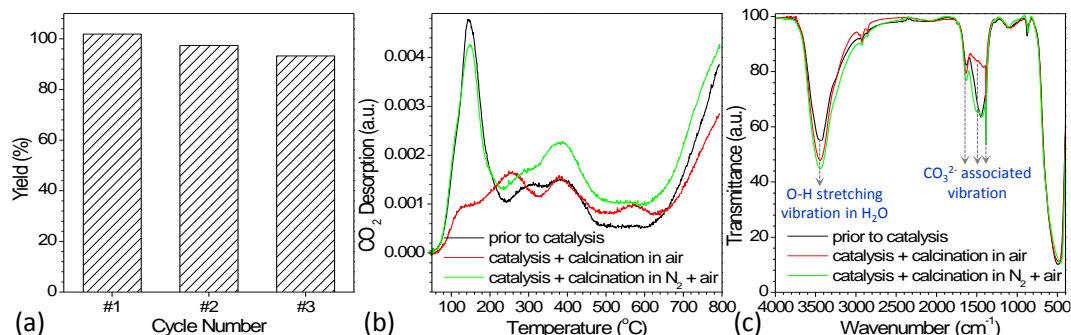


Figure 7. (a) Reuse of trapezoidal MgO after calcination at 550 °C in a N₂ atmosphere and in air, respectively (Note: reaction temperature, 90 °C; reaction time, 2 h; the ratio between glycerol and dimethyl carbonate, 1:3); (b) CO₂-TPD profiles and (c) FT-IR spectrum of the generated MgO prior to catalysis, after catalysis and calcination at 550 °C for 3 h in air and after catalysis and calcination at 400 °C for 3 h in a N₂ atmosphere followed by calcination at 550 °C for 3 h in air.

Various morphologies of micro-sized MgO particles have been prepared by a facile precipitation method via the reaction between Mg(NO₃)₂ and Na₂C₂O₄ or Na₂CO₃ under different reaction temperatures and stirring times. Their catalytic activities were investigated for the synthesis of glycerol carbonate from the glycerol transesterification with dimethyl carbonate. The results demonstrated that in contrast to the MgO with rod-like, spherical, flower-like and nest-like structures, trapezoidal MgO exhibited a superior catalytic performance in production of glycerol carbonate. This fact revealed that the production of glycerol carbonate was highly dependent on the morphology of used MgO. We also found that the developed trapezoidal MgO had a lower specific surface area, bigger crystallite size, weaker surface basicity and less Mg atom vacancies in its structure compared to others. After investigating the influences of experimental conditions on the yield of glycerol carbonate, it was found that the catalyst amount, solvent, reaction temperature and the ratio between glycerol and dimethyl carbonate were responsible for the reaction efficiency. Furthermore, the developed MgO catalyst could be recycled three times after first calcination at 400 °C in a N₂ atmosphere followed by calcination at 550 °C in air, and the catalytic activity was closely related to the weak basic site occurred at 150 °C in CO₂-TPD profile and the CO₃²⁻ stretching vibration around 1448 cm⁻¹. We believe that these knowledge is crucial not only in developing high-efficiency MgO catalyst for production of glycerol carbonate, but also in better understanding the correlation between the catalytic activities of the MgO with different morphologies and their physicochemical properties.

Conflicts of interest

There are no conflicts to declare.

Acknowledgements

The authors would like to acknowledge funding support from the National Natural Science Foundation of China (Nos. 21575112, 21777128 and 21705125) and Shaanxi S&T Research Development Project of China (No. 2016GY-231).

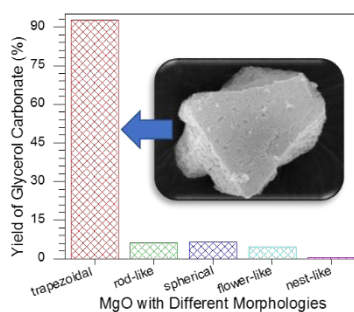
†Electronic Supplementary Information (ESI) available: [FT-IR spectra of the products from different experimental conditions, and photographic images of the collected products after annealing at 400 °C]. See DOI: 10.1039/x0xx00000x

Address, School of Chemistry and Chemical Engineering, Xi'an Shiyou University, Xi'an 710065, China. Fax: +86 29 8838 2693; Tel: +86 29 8838 2694; E-mail: zhangzp0304@gmail.com (Z. Zhang) or tangying78@xsyu.edu.cn (Y. Tang).

References

- M. Pagliaro, R. Ciriminna, H. Kimura, M. Rossi and C. D. Pina, *Angew. Chem. Int. Ed.*, 2007, **46**, 4434-4440.
- M. O. Sonnati, S. Amigoni, E. P. Taffin de Givenchy, T. Darmanin, O. Choulet and F. Guittard, *Green Chem.*, 2013, **15**, 283-306.
- C.-H. Zhou, J. N. Beltramini, Y.-X. Fan and G. Q. Lu, *Chem. Soc. Rev.*, 2008, **37**, 527-549.
- W. K. Teng, G. C. Ngoh, R. Yusoff and M. K. Aroua, *Energy Convers. Manage.*, 2014, **88**, 484-497.
- A. Abbaszaadeh, B. Ghobadian, M. R. Omidkhah and G. Najafi, *Energy Convers. Manage.*, 2012, **63**, 138-148.
- M. J. Climent, A. Corma, P. De Frutos, S. Iborra, M. Noy, A. Velyt and P. Concepción, *J. Catal.*, 2010, **269**, 140-149.
- J. R. Ochoa-Gómez, O. Gómez-Jiménez-Aberasturi, C. Ramírez-López and M. Belsué, *Org. Process Res. Dev.*, 2012, **16**, 389-399.
- F. S. H. Simanjuntak, S. R. Lim, B. S. Ahn, H. S. Kim and H. Lee, *Appl. Catal. A*, 2014, **484**, 33-38.
- A. Takagaki, K. Iwatani, S. Nishimura and K. Ebitani, *Green Chem.*, 2010, **12**, 578-581.
- F. S. H. Simanjuntak, T. K. Kim, D. L. Sang, B. S. Ahn, H. S. Kim and H. Lee, *Appl. Catal. A*, 2011, **401**, 220-225.
- S. Bancquart, C. Vanhove, Y. Pouilloux and J. Barrault, *Appl. Catal. A*, 2001, **218**, 1-11.
- F. S. H. Simanjuntak, V. T. Widyaya, C. S. Kim, B. S. Ahn, Y. J. Kim and H. Lee, *Chem. Eng. Sci.*, 2013, **94**, 265-270.
- M. S. Khayoon and B. H. Hameed, *Appl. Catal. A*, 2013, **466**, 272-281.
- G. Parameswaram, M. Srinivas, B. Hari Babu, P. S. Sai Prasad and N. Lingaiah, *Catal. Sci. Technol.*, 2013, **3**, 3242-3249.
- M. Malyaadri, K. Jagadeeswarai, P. S. Sai Prasad and N. Lingaiah, *Appl. Catal. A*, 2011, **401**, 153-157.
- J. R. Ochoa-Gómez, O. Gómez-Jiménez-Aberasturi, B. Maestro-Madurga, A. Pesquera-Rodríguez, C. Ramírez-López, L. Lorenzo-Ibarreta, J. Torrecilla-Soria and M. C. Villarán-Velasco, *Appl. Catal. A*, 2009, **366**, 315-324.
- M. Kouzu, T. Kasuno, M. Tajika, Y. Sugimoto, S. Yamanaka and J. Hidaka, *Fuel*, 2008, **87**, 2798-2806.
- M. K. Lam, K. T. Lee and A. R. Mohamed, *Biotechnol. Adv.*, 2010, **28**, 500-518.
- H. Hattori, *J. Jpn. Petrol. Inst.*, 2004, **47**, 67-81.
- K. Zhu, J. Hu, C. Kübel and R. Richards, *Angew. Chem.*, 2006, **118**, 7435-7439.
- N. Sutradhar, A. Sinhamahapatra, S. K. Pahari, P. Pal, H. C. Bajaj, I. Mukhopadhyay and A. B. Panda, *J. Phys. Chem. C*, 2011, **115**, 12308-12316.
- F. Wang, N. Ta and W. Shen, *Appl. Catal. A*, 2014, **475**, 76-81.
- J. V. Stark and K. J. Klabunde, *Chem. Mater.*, 1996, **8**, 1913-1918.
- K. J. Klabunde, J. Stark, O. Koper, C. Mohs, D. G. Park, S. Decker, Y. Jiang, I. Lagadic and D. Zhang, *J. Phys. Chem.*, 1996, **100**, 12142-12153.
- X. Zhang, Y. Zheng, H. Yang, Q. Wang and Z. Zhang, *CrystEngComm*, 2015, **17**, 2642-2650.
- Y. Li and W. Shen, *Chem. Soc. Rev.*, 2014, **43**, 1543-1574.
- Z. Zhang, Y. Zheng, Y. Ni, Z. Liu, J. Chen and X. Liang, *J. Phys. Chem. B*, 2006, **110**, 12969-12973.
- Z. Zhang, Y. Zheng, J. Zhang, Q. Zhang, J. Chen, Z. Liu and X. Liang, *Cryst. Growth Des.*, 2007, **7**, 337-342.
- X. Zhang, Y. Zheng, H. Yang, Q. Wang and Z. Zhang, *RSC Adv.*, 2015, **5**, 63034-63043.
- Y. Zheng, X. Zhang, X. Wang, Q. Wang, Z. Bai and Z. Zhang, *CrystEngComm*, 2016, **18**, 2612-2616.
- G. Liu, D. Pan, T. Niu, A. Cao, Y. Yue and Y. Liu, *RSC Adv.*, 2015, **5**, 31637-31647.
- M. M. Nair, S. Kaliaguine and F. Kleitz, *ACS Catal.*, 2014, **4**, 3837-3846.
- M. M. Nair, F. Kleitz and S. Kaliaguine, *ChemCatChem*, 2012, **4**, 387-394.
- V. F. Stone and R. J. Davis, *Chem. Mater.*, 1998, **10**, 1468-1474.
- Y. Takahara, J. N. Kondo, T. Takata, D. Lu and K. Domen, *Chem. Mater.*, 2001, **13**, 1194-1199.
- Z. Bai, Y. Zheng and Z. Zhang, *J. Mater. Chem. A*, 2017, **5**, 6630-6637.
- J. Hu, K. Zhu, L. Chen, C. Kübel and R. Richards, *J. Phys. Chem. C*, 2007, **111**, 12038-12044.
- F. Li, H. Li, L. Wang, P. He and Y. Cao, *Catal. Sci. Technol.*, 2015, **5**, 1021-1034.
- Z. P. Zhang, S. G. Zhang, J. P. Chen, Z. M. Liu and X. M. Liang, *J. Chromatogr. A*, 2006, **1115**, 58-63.
- A. M. Ferrari and G. Pacchioni, *J. Chem. Phys.*, 1997, **107**, 2066-2078.
- E. Giamello, D. Murphy and M. C. Paganini, *Colloids Surf. A*, 1996, **115**, 157-170.
- G. Pacchioni and P. Pescarmona, *Surf. Sci.*, 1998, **412-413**, 657-671.
- A. J. Tench and P. Holroyd, *Chem. Commun.*, 1968, **4**, 471-473.
- P. U. Okoye, A. Z. Abdullah and B. H. Hameed, *Energy Convers. Manage.*, 2017, **133**, 477-485.
- X. Zhang, D. Wang, J. Ma and W. Wei, *Catal. Lett.*, 2017, **147**, 1181-1196.
- X. Wang, P. Zhang, P. Cui, W. Cheng and S. Zhang, *Chin. J. Chem. Eng.*, 2017, **25**, 1182-1186.
- X. Song, Y. Wu, F. Cai, D. Pan and G. Xiao, *Appl. Catal. A*, 2017, **532**, 77-85.
- M. Varkolu, D. R. Burri, S. R. R. Kamaraju, S. B. Jonnalagadda and W. E. Van Zyl, *J. Porous Mater.*, 2016, **23**, 185-193.

For Table of Contents Figure Only



Trapezoidal MgO has been developed for transesterification of glycerol and dimethyl carbonate with a glycerol carbonate yield more than 99%.